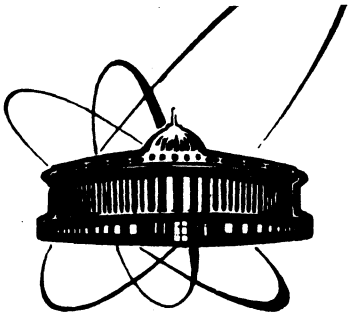

ОБЪЕДИНЕННЫЙ
ИНСТИТУТ
ЯДЕРНЫХ
ИССЛЕДОВАНИЙ
ДУБНА

E1-90-328

ELASTIC SCATTERING OF ANTIPROTONS ON ^{4}He AT 600 MeV/c

Submitted to "Ядерная физика"

1990

Yu.A.Batusov, S.A.Bunyatov, I.V.Falomkin, G.B.Pontecorvo,
A.M.Rozhdestvensky, M.G.Sapozhnikov, V.I.Tretyak
Joint Institute for Nuclear Research, Dubna

F.Balestra, S.Bossolasco, M.P.Bussa, L.Busso, L.Fava, L.Ferrero, A.Maggiora,
D.Panzieri, G.Piragino, R.Piragino, F.Tosello
Istituto di Fisica Generale "A.Avogadro", University of Torino and INFN —
Sezione di Torin, Italy

G.Bendiscioli, V.Filippini, A.Rotondi, P.Salvini, A.Venaglioni
Dipartimento di Fisica Nucleare e Teorica, University of Pavia and INFN —
Sezione di Pavia, Italy

A.Zenoni*
EP Division, CERN, Switzerland

C.Guaraldo
Laboratori Nazionali di Frascati dell'INFN, Frascati, Italy

F.Nichitiu
Institute for Atomic Physics, Bucharest, Romania

E.Lodi Rizzini
Dipartimento di Automazione Industriale, University of Brescia, Brescia,
and INFN — Sezione di Pavia, Pavia, Italy

A.Haatuft, A.Halsteinslid, K.Myklebost, J.M.Olsen
Physics Department, University of Bergen, Bergen, Norway

F.O.Breivik, T.Jakobsen, S.O.Sørensen
Physics Department, University of Oslo, Oslo, Norway

---

* On leave of absence from INFN, Sezione di Pavia, Pavia, Italy

The elastic scattering of antiprotons on light nuclei provides valuable information for investigation of the antiproton-nucleus interaction, for example, for determining the parameters of the antiproton-nucleus potential. Since a reliable description of the elastic scattering is a necessary condition for any adequate model of $\bar{p}A$ -scattering, any new information on the differential elastic scattering cross sections serve as a test for the various models of $\bar{p}A$ -interaction. Besides this, the data on elastic scattering on the lightest nuclei can be used for determining the parameters of the elementary amplitude of antiproton interaction with neutrons which, owing to the absence of good antineutron beams, are not well known.

At present data are available on the elastic scattering of antiprotons on deuterium [1,2], on ^{12}C, ^{40}Ca and ^{208}Pb at 300 and 600 MeV/c [3,4], and on ^{16}O and ^{18}O at 600 MeV/c [5] as well. We have measured the differential cross section of elastic scattering of antiprotons on ^{4}He nuclei at 607.7 MeV/c (T_{kin}= 179.6 MeV). No data on $\bar{p}^{4}He$ elastic scattering at intermediate energies are exist. Earlier we have published the data on the cross sections for antiproton annihilation and inelastic breakup of ^{4}He [6,7].

1. THE EXPERIMENTAL APPARATUS; SCANNING AND MEASUREMENT OF EVENTS

Measurements were performed in the LEAR antiproton beam at CERN using a streamer chamber placed in a magnetic field. The LEAR antiproton beam is characterized by high intensity (10^{5}-10^{6} $\bar{p}$/sec), small momentum spread ($\Delta p/p \approx 10^{-3}$) and total absence of any contamination of pions and kaons whatsoever. The beam is $\approx$ 1 cm in diameter.

The experimental setup is shown in Fig.1. The apparatus was triggered by coincidence signals from the counters C2 and C4 and anticoincidence signals from the counters of the "live" collimator C1 and C3 and from the counter C5 situated after the chamber. Therefore, a trigger occurred, when an antiproton entered the chamber , but did not hit counter C5 at the exit window.

The (90x70x18) cm^3 streamer chamber, operated in the self-shunting mode [8], was filled with helium at atmospheric pressure. The chamber was placed in a magnetic field of 0.8 T. A detailed description of the experimental apparatus can be found in ref. [9].

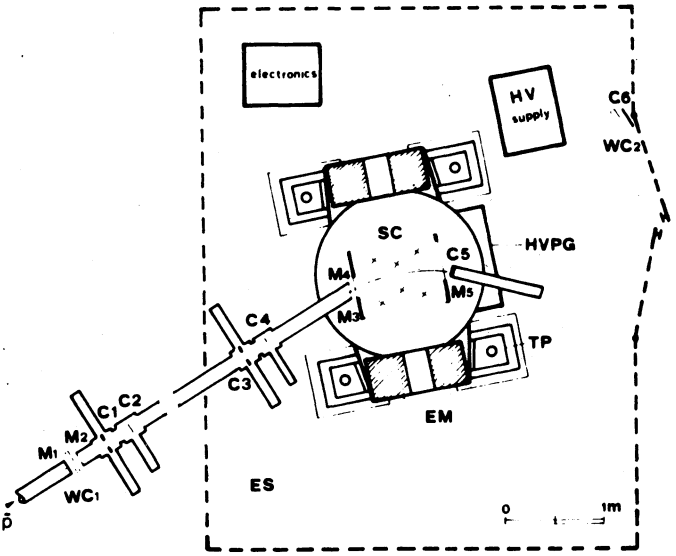

Fig.1 Layout of the experimental apparatus. EM - electromagnet; SC - streamer chamber; HVPG - high voltage pulse generator; TP - pulse generator; TP - travelling platform; ES - electrostatic screening; WC_{1-2} - wire chambers; C_{1-6} - scintillation counters; M_{1-5} - thin walls.

The sensitive volume of the streamer chamber was photographed using two cameras with parallel optical axes 280 mm apart. Each photograph represented a picture of only a single antiproton interaction event with helium.

Approximately 10^5 pictures were scanned in search of elastic scattering events. In all ≈ 3500 two-prong events were found, which were treated as candidates to elastic scattering events. For reliable recording of events a fiducial region 54 cm long was chosen along the beam direction. Besides this, to avoid difficulties in distinguishing between recoil α-particle tracks directed along the electric field in the chamber and spurious tracks of discharges, we have discarded all events with angles between the vertical direction and the plane determined by recoil nucleus and beam directions $|\vartheta| \leq 30^{\circ}$.

The scanning efficiency was determined from the result of a double scanning of 774 two-prong events. It turned out to be 96%.

Measurements were performed using a PUOS [10] measuring device with a coordinate registration precision of 2.5 μm. 92% of the events

detected in the scanning were successfully measured.

Geometrical reconstruction of the measured events was performed with the aid of program written within the HYDRA system [11]. The geometrical reconstruction procedure was successfully applied to 89% of the events.

The precision with which kinematical characteristics of events depended on four input parameters, with the aid of which the measurement errors were calculated. These parameters were the following measurement errors: of coordinates of the vertex projection, δ_v ; of the last point on the track of a stopping particle, δ_s ; of an arbitrary point on a track projection, δ_p ; and of the length of the reconstructed track of a stopping particle, δ_L. These quantities were obtained from the results of multiple measurements of a set of events under the condition that the calculated errors be equal to the ones determined from repeated measurements. The following input parameters were obtained: δ_v = 0.05 cm, δ_s = 0.17 cm, δ_p = 0.14 cm, δ_L = 0.70 cm.

In Fig. 2 the momentum distribution is shown for the beam antiprotons. The average momentum in this distribution is 604.4 ± 4.9 MeV/c. This value is in good agreement with the nominal beam momentum (607.7 ± 1.4) MeV/c.

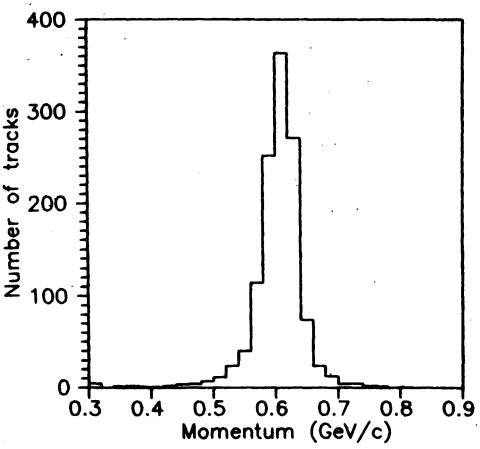

Fig.2.
Measured momentum distribution of beam antiprotons.

2. IDENTIFICATION OF ELASTIC SCATTERING EVENTS

Among the two-prong events with a single negatively charged particle, that were chosen for selecting elastic scattering events, there are also present background events of annihilationless breakup

reactions such as

$$\bar{p} + {}^4He \longrightarrow \bar{p} + n + {}^3He \qquad (2.1)$$

and of annihilation reactions on a neutron with the production of a single $\pi^-(K^-)$- meson and several neutral pions (kaons) such as the following:

$$\bar{p} + {}^4He \longrightarrow \pi^- + {}^3He + m\,\pi^o \qquad (2.2)$$

$$\bar{p} + {}^4He \longrightarrow K^- + K^o + {}^3He + m\,\pi^o, \qquad (2.3)$$

where $m = 0,1,\ldots$.

For identification of elastic scattering events we compared the characteristics of the secondary particles (momentum, scattering angle, range etc.) for each event with the corresponding quantities calculated assuming elastic scattering kinematics. The following criteria were adopted :

1) Angular correlations. The correspondence between the angle of the recoil nucleus and the expected value.

2) Coplanarity. Since elastic scattering events are coplanar, the computed coplanarity angle must be zero. The coplanarity angle is defined as the angle between the incident antiproton track and the plane in which lie the recoil nucleus and the secondary negative particle tracks.

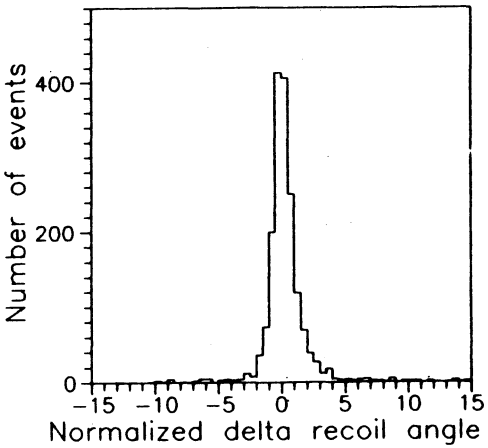

Fig.3. Distribution of events over normalized difference $(\theta_{exp} - \theta_{th}) / \sigma(\theta)$ between measured, θ_{exp}, and calculated, θ_{th}, values of the angle of the recoil nucleus. θ_{th} was calculated from the measured antiproton scattering angle, assuming elastic scattering kinematics. $\sigma(\theta)$ is the experimental measurement error.

3) Correspondence between the measured path of the recoil nucleus and its calculated value. This criterion was applied for recoil nuclei stopping in the chamber. When the recoil nucleus did not stop in the

chamber, its measured momentum was compared with its expected value. 4) Correspondence between the measured momentum of the scattered antiproton and its computed value.

An event was considered elastic, if all the criteria were satisfied within three standard measurement deviations. The most restrictive criterion turned out to be the first one, i.e. taking into account recoil nucleus angular correlations, it was satisfied by 89.8% of all the measured events. (For comparison, the second criterion alone was satisfied by 91.9%, the third by 94.2% and the fourth by 96.3% of all events). In Fig.3 the distribution of the difference $\Delta\theta = (\theta_{exp} - \theta_{th}) / \sigma(\theta)$ is shown,where θ_{exp} and θ_{th} are the measured and calculated recoil angles,respectively,and $\sigma(\theta)$ is the measurement error.

As a result, 84.1 % of the two-prong events satisfying all four criteria were identified as elastic scattering events (1607 events).

For estimation of the background from inelastic scattering the simulation of the reactions (2.1)-(2.3) was performed . It turned out that only 0.5% of the background reaction events satisfied the adopted criteria. We note that for identification of elastic scattering the background conditions were quite favorable, since at our energy the cross section of reaction (2.1) amounts to 4.2 ± 1.3 mb [7] and of reactions (2.2) and (2.3) to 9.3 ± 1.4 mb [6], which is nearly by an order of magnitude lower, than the elastic scattering cross section (see below). Besides this, the elastic scattering events are mainly concentrated at small scattering angles ($\theta_{cm} < 20^{o}$), which is certainly not true for the inelastic events [7].

3. EVALUATION OF THE DIFFERENTIAL CROSS SECTIONS

Antiprotons scattered at small angles could hit the anticoincidence counter C5 (see Fig.1),resulting in the event not being recorded. The dependence of the registration efficiency ε_{C5} upon the $\bar{p}$ scattering angle is presented in Fig.4. This efficiency depends not only on the scattering angle but also on the position of the interaction vertex inside the fiducial volume. So, for evaluation of ε_{C5} we performed simulation of elastic events distributed throughout the entire fiducial volume 54 cm long. The loss of events due to scattered antiprotons hitting the anticoincidence counter C5 was taken into account by introduction of a weight $W_i = 1/ \varepsilon_{C5}(i)$ for each event of scattering angle θ_i . For calculation of the cross section events were utilized with scattering angles corresponding to an efficiency ε_{C5} not lower than 80%.

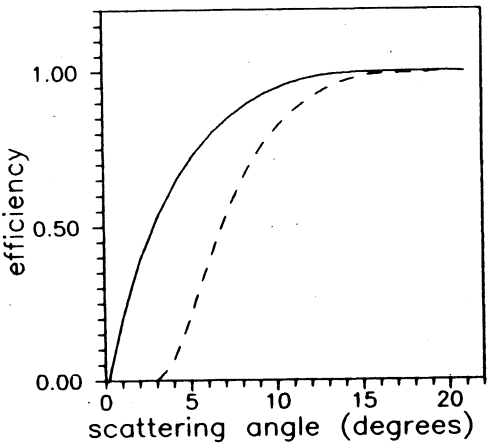

Fig.4. Dependence of registration efficiency, due to the presence of counter C5, on the elastic scattering angle of the $\bar{p}$. The curves correspond to registration efficiencies calculated for two different diameters of counter C5: 8 cm (solid line) and 13 cm (dashed line). 77% of the experimental data were obtained with an 8 cm C5 counter.

Differential cross sections were calculated by the formula

$$\frac{d\sigma}{d\Omega} = \frac{\sigma_o \cdot \sum_i W_i}{\varepsilon \cdot C \cdot \Delta\Omega}, \qquad (3.1)$$

where $\sigma_o = (N_{in} \cdot \rho \cdot L)^{-1}$ ($N_{in} \simeq 23 \cdot 10^6$ is the number of antiprotons that traversed the target, ρ is the amount of ^{4}He nuclei per unit volume, L = 54.6 cm is the mean length of the path travelled by $\bar{p}$ through the fiducial volume), ε is the overall efficiency of scanning, measurements and geometrical reconstruction of events (ε=0.79), C = 2/3 is a coefficient taking into account the cut in the recoil nucleus direction (see section 1), W_i are the weights of events in the angular interval $\Delta\Omega$.

The obtained differential cross sections are presented in Table.

For determination of the total $\bar{p}^4$He elastic scattering cross section the differential cross section was approximated by the following expression:

$$d\sigma/d\Omega = | F_{Coul}(\theta) + F_{nucl}(\theta) |^2 , \qquad (3.2)$$

where the nuclear amplitude $F_{nucl}(\theta)$ was taken in the form:

$$F_{nucl}(\theta) = \sigma_{tot}^{k(i+\rho)} \cdot \exp(-B\, t/2) \cdot (1 - t/t_o)/4\pi . \qquad (3.3)$$

Here k is the c.m. momentum of $\bar{p}$, $t = 2k^2(1 - \cos\theta)$ is the square momentum transfer, σ_{tot} is the total $\bar{p}^4$He scattering cross section, ρ=Re $F_{nucl}(0)$/Im $F_{nucl}(0)$, B is the slope parameter in $d\sigma/d\Omega$, t_o is a complex parameter ,corresponding to the zero of the scattering amplitude,and Re t_o is determined by the position of the minimum in $d\sigma/d\Omega$, while Im t_o is related to the value of $d\sigma/d\Omega$ at the minimum.

Table. Differential cross sections of elastic $\bar{p}^4$He scattering (in the centre-of-mass system). In the column θ_{cms} indicated is the weighted mean value of the cms scattering angle in the respective angular bin

θ_{cms} (deg)	Angular bin	$d\sigma/d\Omega$ (mb/sr)	θ_{cms} (deg)	Angular bin	$d\sigma/d\Omega$ (mb/sr)
9.0	(8.,10.)	369.115 ± 32.373	32.7	(32.,35.)	6.177 ± 1.498
10.9	(10.,12.)	345.906 ± 25.095	36.2	(35.,38.)	1.330 ± 0.665
13.0	(12.,14.)	260.394 ± 19.302	39.3	(38.,41.)	0.620 ± 0.439
15.0	(14.,16.)	221.025 ± 16.250	42.7	(41.,44.)	1.448 ± 0.647
16.9	(16.,18.)	163.111 ± 13.018	42.7	(41.,44.)	1.448 ± 0.647
19.0	(18.,20.)	117.354 ± 10.373	45.0	(44.,47.)	2.221 ± 0.785
20.9	(20.,22.)	83.291 ± 8.329	49.1	(47.,52.)	1.092 ± 0.413
23.0	(22.,24.)	62.183 ± 6.867	54.0	(52.,57.)	1.020 ± 0.385
25.1	(24.,26.)	48.736 ± 5.825	59.6	(57.,62.)	0.410 ± 0.237
27.0	(26.,28.)	39.610 ± 5.071	63.6	(62.,67.)	1.053 ± 0.372
29.0	(28.,30.)	15.177 ± 3.035	68.5	(67.,77.)	0.127 ± 0.090
30.7	(30.,32.)	12.106 ± 2.642	86.2	(77.,97.)	0.059 ± 0.042
			107.8	(97.,117.)	0.062 ± 0.044

The Coulomb amplitude $F_{Coul}(\theta)$ was evaluated taking into account the finite dimensions of the ^{4}He nucleus and of the antiproton applying the method described in ref.[12]:

$$F_{Coul}(\theta) = F_{point} - F_{Born}\cdot(1 - f_p(t)\cdot f_{He}(t)), \qquad (3.4)$$

where the Coulomb scattering amplitude on a pointlike particle, F_{point}, is

$$F_{point} = F_{Born}\cdot \exp(-(2i\,C\,\zeta + \zeta\,\ln(\,(1-\cos\theta\,)/2))). \qquad (3.5)$$

Here C is the Euler constant, C = 0.5772 , ζ is the Coulomb parameter:

$$\zeta = \frac{Z_1 \cdot Z_2 \cdot \alpha \, (S - (m^2 + M^2))}{[S - (m + M)^2]^{1/2} \cdot [S - (m - M)^2]^{1/2}} , \qquad (3.6)$$

α = 1/137 , S is the total energy of the $\bar{p}^4$He system, and m and M are the $\bar{p}$ and ^{4}He masses, respectively,

$$F_{Born} = - 2 \cdot \zeta \cdot k \; / \; t. \qquad (3.7)$$

The helium and the antiproton form factors were taken in the Gaussian form :

$$f_p(t) = \exp \, (- r^2 \cdot t/6)$$
$$f_{He}(t) = \exp \, (- R^2 \cdot t/6), \qquad (3.8)$$

where r = 0.8 fm, R = 1.67 fm .

To determine the parameters of the amplitude $F_{nucl}(\theta)$, we proceeded in two steps. First, we considered all parameters in (3.3) for $F_{nucl}(\theta)$ to be free parameters and determined them by fitting the differential cross section in the whole angular range of our measurements. The quality of the fit is put in evidence in Fig.5 , it turns out that χ^2/NDF = 1.18 . However, the parameters σ_{tot}, ρ, and B are correlated. To reduce the correlation effects we try to fix some of the parameters by applying additional experimental information. Thus, using $F_{nucl}(\theta)$ from the best fit, we can determine the total elastic cross section:

$$\sigma_{el} = \int |F_{nucl}(\theta)|^2 \, d\Omega = (120.9 \pm 2.5) \text{ mb}. \qquad (3.9)$$

From (3.9) one may obtain the total $\bar{p}^4$He interaction cross section:

$$\sigma_{tot} = \sigma_R + \sigma_{el} = (360.1 \pm 5.6) \text{ mb} \quad . \qquad (3.10)$$

Here σ_R is the cross section of all inelastic $\bar{p}^4$He reactions measured in our previous work, σ_R = 239.2 ± 5.0 mb [6].

For better determination of the ρ and B parameters that depend on the F_{nucl} behavior in the forward direction we fixed in (3.3) the value of σ_{tot} from (3.10) and fitted $d\sigma/d\Omega$ only for a small scattering angles region ($\theta \leq 22^o$) by (3.2) , but without the factor $(1-t/t_o)$. The following results were obtained:

$$B = 58.7 \pm 1.4 \text{ (GeV/c)}^{-2},$$
$$\rho = 0.22 \pm 0.05 \; . \qquad (3.11)$$

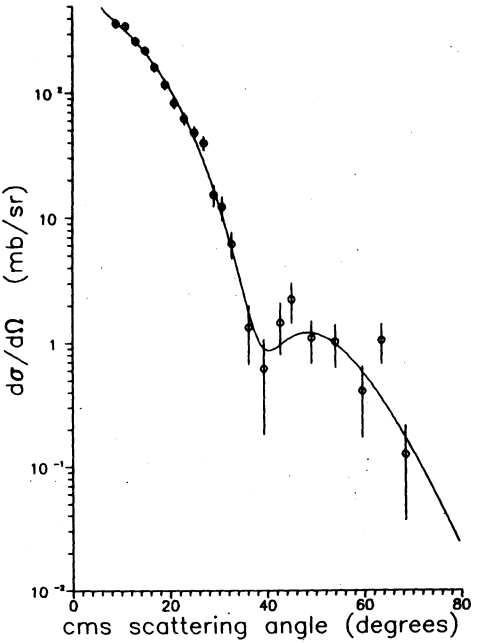

Fig.5.

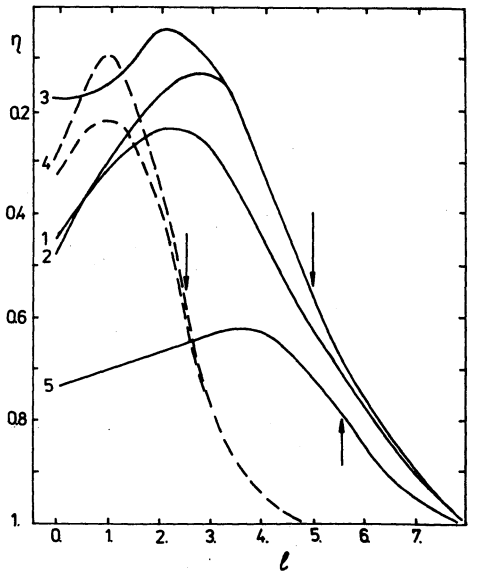

Fig.6.

Fig.5. Differential elastic $\bar{p}^4$He cross section at 607.7 MeV/c. The line corresponds to a fit by the formula (3.2).

Fig.6. The inelasticity parameter η versus angular momentum l. Curve 1 - η obtained with the amplitude (3.3) without the factor $(1 - t/t_o)$; curve 2 corresponds to a fit with the amplitude (3.3) (Im $t_o < 0$); curve 3 - the same as curve 2, but with Im $t_o > 0$; curves 4 - for π^{-4}He scattering with two zeros in the amplitude, the corridor contains all 4 solutions; curve 5 - for p^4He scattering with 4 zeros in the amplitude (all Im $t_i > 0$ and $\theta_{max} < 120^o$). Arrows indicate the $l_{max} \approx k\,(R_{He} + R_p)$, where R_{He} and R_p are the charge radii of ^{4}He and of the scattered particle, respectively.

4. DISCUSSION OF THE OBTAINED DATA

Knowledge of the parameters of the amplitude $F_{nucl}(\theta)$ in (3.3) allows to perform partial wave projection and to determine the

scattering phases δ_l and the inelasticity parameters η_l:

$$f_l = k \frac{2l+1}{2} \int F_{nucl}(\theta)\, P_l(\cos\theta)\, d(\cos\theta), \qquad (4.1)$$

where $f_l = (\eta_l \exp(2i\delta_l)-1)/2i$ are the spin-averaged partial amplitudes and $P_l(\cos\theta)$ are Legendre polynomials.

The fit for determining the amplitude was performed for the entire angular interval with σ_{tot} set equal to the value given by eq.(3.10) and, also, with and without the factor $(1-t/t_o)$. The same fit was done for the elastic scattering on ^{4}He of pions [13] and also of protons [14] at comparable energies.

In Fig. 6 the inelasticity parameter η_l (from eq. 4.1) is plotted versus angular momentum l for antiprotons (curves 1 - 3), pions (the corridor denoted by 4) and protons (curve 5). We recall that ,if only the elastic channel is open, $\eta_l = 1$. It is clearly seen that π^4He scattering exhibits the characteristic maximum in the P-wave, in p^4He elastic scattering none of the partial waves are singled out in such a manner.

From the results presented in Fig. 6 it follows that at our energy the P,D and F -waves are dominant,although a large number of partial waves, practically up to l=6-7, is required for describing the $\bar{p}$ ^{4}He elastic scattering. As l increases from l=3 to l=6-7, the inelasticity decreases ($\eta_l \longrightarrow 1$). Im f_l turns out to be significantly greater than Re f_l. This is typical of hadron scattering in the presence of strong absorption.

The above can also be verified by the analysis of these $\bar{p}$ ^{4}He elastic scattering data in terms of a simple "fuzzy black disk model", i.e. a black disk with a diffuse boundary [15]. This particular model proved very successful in the phenomenological analysis of antiproton elastic scattering on different nuclei [16]. The scattering amplitude for a black disk is given by

$$f(\theta) = kR^2 \frac{J_1(x)}{x}, \qquad (4.2)$$

where $x = 2kR \sin(\theta/2)$.

The effect of surface diffuseness on a black disk is taken into account [15] by the function :

$$D(\theta) = \exp(-\Delta^2 k^2 \sin^2(\theta/2)) \qquad (4.3)$$

and therefore the scattering cross section is given by

$$d\sigma/d\Omega = (kR^2)^2 \frac{J_1^2(x)}{x^2} \exp(-2\Delta^2 k^2 \sin^2(\theta/2)). \qquad (4.4)$$

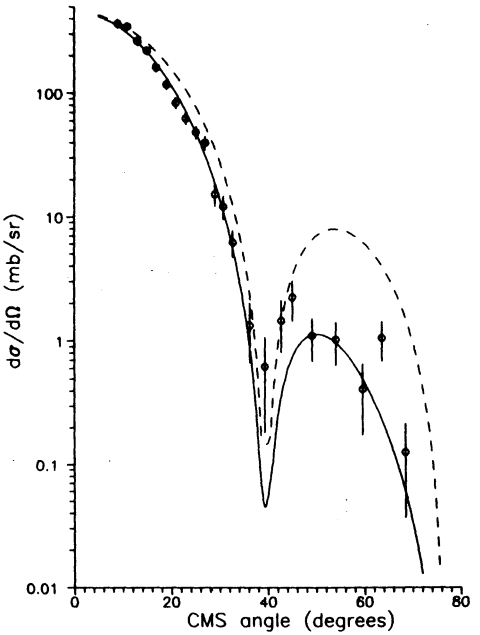

Fig.7

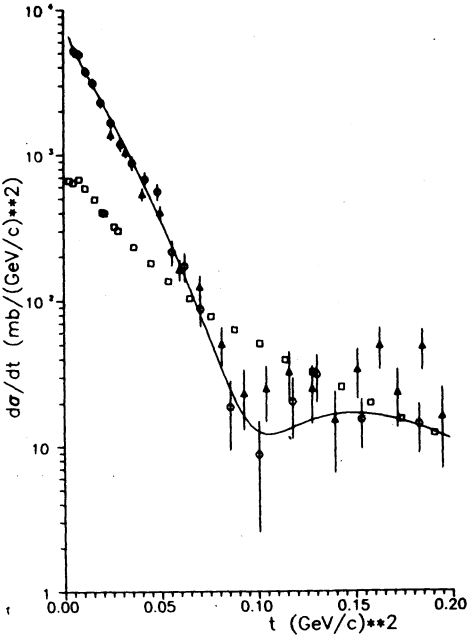

Fig.8

Fig.7. Black disk fit of the differential elastic $\bar{p}^4$He cross section. Solid curve - best fit with diffuseness parameter Δ = 0.95 fm. Dashed line - calculations for a black disk with sharp edge (Δ=0).

Fig.8. Comparison of differential cross section $d\sigma/dt$ for $\bar{p}^4$He elastic scattering at T=180 MeV (circles) with $d\sigma/dt$ for p^4He elastic scattering at T=200 MeV (squares) [14] and with that for π^{-4}He at T=174 MeV (triangles) [13].

Two parameters are present in (4.4): R, the black disk radius, and the diffuseness parameter Δ. The radius R depends essentially on the location of the minima in the $d\sigma/d\Omega$ and Δ depends on the overall slope of the angular distribution. With the aid of a fit of $d\sigma/d\Omega$ by (4.4) we averaged the calculated cross sections over bins of the angular distribution. The typical black disk sharp minima are thus smoothed out. The result of the fit is shown in Fig.7, where the solid line shows the result of fitting expression (4.4) and the broken line corresponds to calculation by the black disk formula without a diffuseness function. One can see that even the naive black disk approach provides a not too bad description of the experimental differential cross section. The addition of the realistic assumption

concerning the diffuseness results in quite a good agreement with the experimental data, practically the same as in the case of antiproton elastic scattering on heavy nuclei [16].

The obtained value R = (2.38 ± 0.02) fm is in good agreement with the value following from the simple parametrization $R = 1.5A^{1/3}$ found in ref. [13] for heavier nuclei. The diffuseness parameter Δ = (0.95 ± 0.03) fm turned out to be the same as for other nuclei ($\Delta \sim 1$ fm) [13]. This is a consequence of the large effective radius of $\bar{p}A$ interaction.

It is instructive to compare the elastic scattering of antiprotons with that of pions. In Fig.8 shown are the differential cross sections of antiproton, pion and proton elastic scattering on ^{4}He versus the momentum transfer t. One can immediately observe the striking similarity between the pion and antiproton $d\sigma/dt$ distributions. This, at first sight, unexpected result merely reflects the fact that in the region of the Δ_{33} - resonance the inelastic cross section of π^4He interaction approaches its maximum (approximately 220 mb [17]) which incidentally coincides with σ_{inel} for $\bar{p}^4$He interaction (σ_{inel} = 239.2 ± 5.0 mb [6]). The equally strong absorption exhibited in the case of pions and antiprotons, with inelastic cross sections that happen to be the same, leads to similar differential elastic scattering cross sections. The above similarity should be destroyed, for instance, at low energies where the πA cross section decreases, whereas the $\bar{p}$A cross section increases.

CONCLUSIONS

We have measured the differential cross section for antiproton elastic scattering on ^{4}He at 607.7 MeV/c. The angular dependence of $d\sigma/d\Omega$ exhibits the diffraction pattern typical of scattering on a strongly absorbing disk. Simply taking into account diffuseness of the disk provides good agreement of calculations with the experimental data.

From the measured total elastic cross section σ_{el} = (120.9 ± 2.5) mb and the $\bar{p}^4$He reaction cross section, σ_R , measured previously, the total $\bar{p}^4$He interaction cross section is determined to be σ_{tot} = (360.1 ± 5.6) mb . From a fit of the forward scattering data the parameter ρ=Re $F_{nucl}(0)$/Im $F_{nucl}(0)$ turns out to be ρ = 0.22 ± 0.05, and the slope parameter is B = 58.7 ± 1.4 $(GeV/c)^{-2}$.

Partial wave projection of antiproton- nucleus amplitude reveals that the P,D and F -waves are dominant, although a large number of partial waves, practically up to l=6-7, is required for describing the

$\bar{p}$ ^{4}He elastic scattering at our energy. The imaginary parts of the partial amplitudes are significantly greater, than the real ones. This is characteristic of hadron scattering in the presence of strong absorption.

The LEAR and South Hall CERN Area teams are gratefully acknowledged for their continuous support during data taking. The authors are also grateful to V.V.Bogdanova, G.A.Kul'kova, M.N.Shelaeva and L.A.Vasilenko for their indispensable help in scanning and measuring the experimental material.

REFERENCES

1. Bizzarri R. et al., Nuov.Cim., 1974, v.22A, p.225.
2. Bruge G. et al., Phys.Rev., 1988, v.C37, p.1345.
3. Garreta D. et al., Phys.Lett., 1984, v.B135, p.266.
4. Garreta D. et al., Phys.Lett., 1984, v.B149, p.64;
5. Bruge G. et al., Phys.Lett.,1986, v.B169, p.14.
6. Balestra F. et al., Nuov.Cim. 1988, v.100A, p.323.
7. Balestra F. et al., Phys.Lett, 1984, v.149B, p.69; 1987, v.194B, p.343.
8. Falomkin I.V. et al., Nucl. Instr. and Meth., 1967, v.53, p.266.
9. Balestra F. et al., Nucl.Instr. and Meth., 1985, v.234, p.30.
   Balestra F. et al., Nucl.Instr. and Meth., 1987, v.A257, p.114.
10. Ermolaev V.F. et al., JINR 10-5973, Dubna, 1971 (in russian).
11. Böck R.K. and Zoll J., JINR D10,11-8450, Dubna, 1974.
12. Das K.M., Deo B.B, Phys.Rev., 1982, v.C26, p.211.
13. Shcherbakov Yu.A. et al., Nuov. Cim., 1976, v.31A, p.249.
14. Moss G.A. et al., Phys.Rev., 1980, v.C21, p.1932.
15. Inopin E.V., Berezhnoy Yu.A., Nucl.Phys., v.63, 1965, p.689.
16. Lichtenstadt J. et al., Phys.Rev. 1985, v.C32, p.1096.
17. Binon F. et al., Nucl.Phys.,1978, v.A298, p.499.

Received by Publishing Department
on May 11, 1990.

SUBJECT CATEGORIES
OF THE JINR PUBLICATIONS

Index	Subject
1.	High energy experimental physics
2.	High energy theoretical physics
3.	Low energy experimental physics
4.	Low energy theoretical physics
5.	Mathematics
6.	Nuclear spectroscopy and radiochemistry
7.	Heavy ion physics
8.	Cryogenics
9.	Accelerators
10.	Automatization of data processing
11.	Computing mathematics and technique
12.	Chemistry
13.	Experimental techniques and methods
14.	Solid state physics. Liquids
15.	Experimental physics of nuclear reactions at low energies
16.	Health physics. Shieldings
17.	Theory of condenced matter
18.	Applied researches
19.	Biophysics

WILL YOU FILL BLANK SPACES IN YOUR LIBRARY?

You can receive by post the books listed below. Prices — in US $, including the packing and registered postage.

D13-85-793	Proceedings of the XII International Symposium on Nuclear Electronics, Dubna, 1985.	14.00
D4-85-851	Proceedings of the International School on Nuclear Structure Alushta, 1985.	11.00
D1,2-86-668	Proceedings of the VIII International Seminar on High Energy Physics Problems, Dubna, 1986 (2 volumes)	23.00
D3,4,17-86-747	Proceedings of the V International School on Neutron Physics. Alushta, 1986.	25.00
D9-87-105	Proceedings of the X All-Union Conference on Charged Particle Accelerators. Dubna, 1986 (2 volumes)	25.00
D7-87-68	Proceedings of the International School-Seminar on Heavy Ion Physics. Dubna, 1986.	25.00
D2-87-123	Proceedings of the Conference "Renormalization Group-86". Dubna, 1986.	12.00
D4-87-692	Proceedings of the International Conference on the Theory of Few Body and Quark-Hadronic Systems. Dubna, 1987.	12.00
D2-87-798	Proceedings of the VIII International Conference on the Problems of Quantum Field Theory. Alushta, 1987.	10.00
D14-87-799	Proceedings of the International Symposium on Muon and Pion Interactions with Matter. Dubna, 1987.	13.00
D17-88-95	Proceedings of the IV International Symposium on Selected Topics in Statistical Mechanics. Dubna, 1987.	14.00
E1,2-88-426	Proceedings of the 1987 JINR-CERN School of Physics. Varna, Bulgaria, 1987.	14.00
D14-88-833	Proceedings of the International Workshop on Modern Trends in Activation Analysis in JINR. Dubna, 1988	8.00
D13-88-938	Proceedings of the XIII International Symposium on Nuclear Electronics. Varna, 1988	13.00
D10-89-70	Proceedings of the International School on the Problems of Use of Computers in Physical Research. Dubna, 1988	8.00
D9-89-52	Proceedings of the XI All-Union Conference on Charged Particle Accelerators. Dubna, 1988 (2 volumes)	30.00
D4,6,15-89-638	Proceedings on the International Conference on Selected Topics in Nuclear Structure. Dubna, 1989	14.00

Orders for the above-mentioned books can be sent at the address:
Publishing Department, JINR
Head Post Office, P.O.Box 79 101000 Moscow, USSR

Батусов Ю.А. и др. E1-90-328

Упругое рассеяние антипротонов на ^{4}He при 600 МэВ/с

Измерено дифференциальное сечение упругого рассеяния антипротонов на ^{4}He при импульсе 607,7 МэВ/с. Определено полное сечение упругого рассеяния σ_{el} = (120,9 ± 2,5) мб и полное сечение взаимодействия σ_{tot} = (360,1 ± 5,6)мб. Парциально-волновой анализ показывает, что рассеяние идет, в основном, из P, D и F состояний. Угловая зависимость $d\sigma/d\Omega$ обнаруживает поведение типичное для дифракции на сильно поглощающем диске. Учет размытости края черного диска обеспечивает хорошее согласие расчетов с экспериментальными данными.

Работа выполнена в Лаборатории ядерных проблем ОИЯИ.

Препринт Объединенного института ядерных исследований. Дубна 1990

Batusov Yu.A. et al. E1-90-328

Elastic Scattering of Antiprotons on ^{4}He at 600 MeV/c

The differential cross section for antiproton elastic scattering on ^{4}He at 607.7 MeV/c is measured. The total elastic cross section σ_{el} = (120.9 ± 2.5) mb and the total $\bar{p}^4$He interaction cross section σ_{tot} = (360.1 ± ± 5.6) mb are determined. Partial wave analysis reveals that the P, D and F-waves are dominant in the scattering. The angular dependence of $d\sigma/d\Omega$ exhibits the diffraction pattern typical of scattering on a strongly absorbing disk. Simply taking into account diffuseness of the disk provides good agreement of calculations with the experimental data.

The investigation has been performed at the Laboratory of Nuclear Problems, JINR.

Preprint of the Joint Institute for Nuclear Research. Dubna 1990